

# An exact axisymmetric spiral solution of the incompressible 3D Euler equations

By LIANG SUN<sup>1,2†</sup>

<sup>1</sup>School of Earth and Space Sciences, University of Science and Technology of China, Hefei, 230026, China.

<sup>2</sup>Dept. of Modern Mechanics, University of Science and Technology of China, Hefei, 230026, China.

(Received 27 August 2018, and in revised form ??)

Spiral structure is one of the most common structures in the nature flows. A general steady spiral solution of incompressible inviscid axisymmetric flow was obtained analytically by applying separation of variables to the 3D Euler equations. The solution, depending on 3 parameters, describes the spiral path of the fluid material element on the Bernoulli surface, whereas some new exact solutions were obtained to be bounded within the whole region. The first one is a continued typhoon-like vortex solution, where there are two intrinsic length scales. One is the radius of maximum circular velocity  $r_m$ , the other is the radius of the vortex kernel  $r_k = \sqrt{2}r_m$ . The second one is a multi-planar solution, periodically in  $z$ -coordinate. Within each layer, the solution is a umbrella vortex similar to the first one. The third one is also a multi-planar solution in  $z$ -coordinate. In each layer, it is a combination of two independent solutions like the Rankine vortex, which is also finite but discontinued for either vertical or horizontal velocity. The fourth one is a multi-paraboloid vortex solution finite for  $z$ -coordinate but infinite for  $r$ -coordinate. Besides, some classical simple solutions (Rankine vortex, Batchelor vortex, Hill spherical vortex, etc.) were also obtained. The above explicit solutions can be applied to study the radial structure of the typhoon, tornados and mesoscale eddies. Both the solutions and approaches used here could also be applied to other complex flows by the Navier-Stokes equations.

---

## 1. Introduction

The exact solutions of the Euler equations for inviscid flow are quite important for understanding how the real fluid will flow. But it is a big problem for solving the Euler equations due to the nonlinearity. Within 2D (two-dimensional) context, the complex potential can effectively solve the irrotational flow by turning the Euler equations to linear ones. For the 2D inviscid flow with vorticity, the vorticity-stream formulation can simplify the problem to a generalized Helmholtz equation (Batchelor 1967). Consequently, some special explicit solutions were obtained after this simplification (Wang 1991; Saffman 1992; Majda & Bertozzi 2002; Wu *et al.* 2006). And Lou *et al.* (2007) also obtained some non-steady solutions from the steady solutions by the general symmetry group theorem.

Within 3D (three-dimensional) flow context, the problem becomes more complex, especially for the 3D flow with vorticity and swirling. The nonlinear advection term make the equations hardly to be solved. If the nonlinear advection term vanishes everywhere at certain conditions, the flow is called the Beltrami flow. Thus the Euler equations could be

† Corresponding Author: Liang Sun, email: sunl@ustc.edu.cn;sunl@ustc.edu.

simplified to linear equations, and some exact solutions might be obtained. The known limited exact solutions of the Euler and Navier-Stokes equations were reviewed in detail by Wang (1991); Shtern & Hussain (1999). Such solutions from simplicity to complexity include concentric flows, parallel flows, linear flows, the generalized Beltrami flows in axisymmetric case (Wang 1991). Among them, the exact solutions for generalized Beltrami flows are the most complex, and they describe swirling flows of widespread technological importance.

Within 3D axisymmetric context, the simplest Beltrami flow is a steady swirling flow, where both the radial velocity and azimuthal velocities are dependent of the radial coordinate  $z$ , but of the axial coordinate  $r$  (Shtern *et al.* 1997). In this case, the Euler equations for the radial velocity, the azimuthal velocity and swirl are decoupled, where the coupling of three velocity components are arbitrarily constructed rather than derived from reasonable boundary conditions. The solutions include the Burgers vortex, the Sullivan vortex (e.g. Wang 1991; Wu *et al.* 2006), and a family of general sink vortices (Shtern *et al.* 1997). Another simple axisymmetrically Beltrami flow is symmetric sink without swirling. Some of them are impingement of two rotating streams, rotational stagnation flow over a plate, the Hill spherical vortex and etc (Wang 1991; Wu *et al.* 2006). Moffatt (1969) also extended the Hill spherical vortex to allow for a swirl with nonzero circumferential velocity that causes a circulation around the  $z$ -axis.

Although the above solutions are helpful, most of the symmetric sink solutions are decoupled and unbounded, except for, e.g., the Hill spherical vortex and its extension. The decoupled and unbounded solutions might be of some limited physical interest. To avoid this arbitrariness and unboundedness, Long (1958, 1961) tried first to obtain the coupled equations for conical similarity swirling vortex, and the Euler equations can be simplified to the Bragg-Hawthorne equation, or the Long-Squire equation (Batchelor 1967; Saffman 1992; Frewer *et al.* 2007). However, such equation is generally nonlinear, no exact explicit solution has been obtained.

In contrast to that, Frewer *et al.* (2007) used Lie-algebras to investigate the Bragg-Hawthorne equation. They found out eight distinct local Bragg-Hawthorne symmetries within five algebras. However, such symmetries are different and even more symmetries than the Euler equations do (Frewer *et al.* 2007). To dispel the inequivalent between them, they need to obtain some additional equations. Even though, they also find only the simple linear Bragg-Hawthorne equation can be solved explicitly (Batchelor 1967; Frewer *et al.* 2007).

As an alternative way to avoid the above disadvantage, we considered to solve the coupled nonlinear Euler equations following the deviation by Batchelor (1967), which is the most complex Beltrami flow with that all the velocity components are dependent on both the radial coordinate  $r$  and the axial coordinate  $z$ . Due to the complexity, the general explicit solution for such flow still lacks even in the recent literatures (Majda & Bertozzi 2002; Wu *et al.* 2006). In this study, we solved the Euler equations by applying separation of variables (Sun 2011). As a result, a general exact spiral solution was presented in §2, some special explicit solutions were given in §3. Discussion and conclusion were respectively given in §4 and in §5.

## 2. General solution

We considered the steady solution of the incompressible Euler equations for axisymmetric flow at present study. It is convenient to use a cylindrical coordinate system  $(r, \theta, z)$  with the velocity components  $(V_r, V_\theta, V_z)$ , and all the velocity components are the functions of  $r$  and  $z$  but  $\theta$ , due to the axisymmetric. As  $V_r = V_r(r, z)$ ,  $V_\theta = V_\theta(r, z)$

and  $V_z = V_z(r, z)$ , the governing equations, including mass-conservation and momentum equations, are

$$\frac{\partial(rV_r)}{\partial r} + \frac{\partial(rV_z)}{\partial z} = 0 \quad (2.1a)$$

$$V_r \frac{\partial V_\theta}{\partial r} + V_z \frac{\partial V_\theta}{\partial z} + \frac{V_r V_\theta}{r} = 0 \quad (2.1b)$$

$$V_r \frac{\partial V_r}{\partial r} + V_z \frac{\partial V_r}{\partial z} - \frac{V_\theta^2}{r} = -\frac{1}{\rho} \frac{\partial p}{\partial r} \quad (2.1c)$$

$$V_r \frac{\partial V_z}{\partial r} + V_z \frac{\partial V_z}{\partial z} = -\frac{1}{\rho} \frac{\partial p}{\partial z} \quad (2.1d)$$

It should be noted that there is no length scale in Eq.(2.1), thus the solution can be uniformly stretched by simply multiplying a complex constant. Batchelor (1967) noted that Eq.(2.1a) and Eq.(2.1b) can be solved through the introduction of the axisymmetric stream function  $\Psi(r, z)$ . We tried to find the solution of the above equations by separation of variables  $\Psi(r, z) = R(r)H(z)$ . One such solution can be written as,

$$V_r = \frac{R(r)}{r} H'(z), \quad V_\theta = \lambda \frac{R(r)}{r} H(z), \quad V_z = -\frac{R'(r)}{r} H(z) \quad (2.2)$$

where ' presents first deviation and  $\lambda$  is a complex constant. In this way, equation (2.1a) and equation (2.1b) are satisfied automatically. The path of a fluid material element can be obtained,

$$\ln r(\theta) = \frac{1}{\lambda} \frac{H'}{H} \theta \quad (2.3a)$$

$$\Psi(r, z) = \text{const.} \quad (2.3b)$$

In  $r-\theta$  plan, it is a logarithmic spiral ( $H' \neq 0$ ), except for  $H' = 0$  (a circle). So we called the solution is spiral solution. In fact, the path is right on a Bernoulli surface given by Eq.(2.3b), on which the streamfunction is defined (Batchelor 1967).

Equation (2.1c) and equation (2.1d) become,

$$\left(\frac{R}{r}\right)\left(\frac{R}{r}\right)' H'^2 - \left(\frac{R}{r}\right)\left(\frac{R'}{r}\right) H H'' - \frac{\lambda^2}{r^3} R^2 H^2 = -\frac{1}{\rho} \frac{\partial p}{\partial r} \quad (2.4a)$$

$$\left(\frac{R'}{r}\right)^2 H H' - \left(\frac{R}{r}\right)\left(\frac{R'}{r}\right)' H H' = -\frac{1}{\rho} \frac{\partial p}{\partial z} \quad (2.4b)$$

Hence, the pressure can be solved from Eq.(2.4b),

$$p(r, z) = \frac{1}{2} \rho H^2 \left[ \left(\frac{R}{r}\right)\left(\frac{R'}{r}\right)' - \left(\frac{R'}{r}\right)^2 \right] - \rho Q(r) \quad (2.5)$$

Substituting Eq.(2.5) into Eq.(2.4a), it yields

$$\left(\frac{R}{r}\right)\left(\frac{R}{r}\right)' H'^2 - \left(\frac{R}{r}\right)\left(\frac{R'}{r}\right) (H H'') - \left(\frac{\lambda^2}{r^3} R^2\right) H^2 = \frac{1}{2} \left[ \left(\frac{R'}{r}\right)^2 - \left(\frac{R}{r}\right)\left(\frac{R'}{r}\right)' \right] H^2 + Q'(r) \quad (2.6)$$

Recall that  $R$  and  $H$  are independent, we can solve the above equation. There are three kind of functions for  $H(z)$  in Eq.(2.6). The first trivial one is  $H = 1$ , any differentiable function  $R(r)$  would be the solution, which we discussed in §3.2.1. Besides, it also yields two kind of non-trivial solutions for  $H(z)$ : a) both  $H'^2$  and  $H H''$  are independent to  $H^2$ , and b) both  $H'^2$  and  $H H''$  are proportion to  $H^2$ . This yields

$$H H'' = \frac{n}{n-1} H'^2, \quad n = 1, 2, \text{ or,} \quad (2.7a)$$

$$HH'' = k^2H^2, \text{ and, } H'^2 = k^2H^2 \pm 4\alpha\beta k^2. \quad (2.7b)$$

where  $k$  and  $\beta$  are two complex constants. The solutions are obtained for  $H(z)$  and  $Q(r)$ ,

$$H(z) = z^n, Q(r) = \frac{1}{2}\left(\frac{R}{r}\right)^2 - (n-1) \int \frac{RR'}{r^3} dr, \text{ or,} \quad (2.8a)$$

$$H(z) = \alpha e^{kz} \pm \beta e^{-kz}, Q(r) = \pm 2\alpha\beta k^2 \left(\frac{R}{r}\right)^2, \quad k^2 \neq 0, \quad (2.8b)$$

Substitution Eq.(2.8) into Eq.(2.6) to eliminate the function for  $z$ , and letting  $\gamma = \lambda^2 + k^2$ , it yields

$$-\frac{2\gamma}{r^3}R^2 = \left[\left(\frac{R'}{r}\right)^2 - \left(\frac{R}{r}\right)\left(\frac{R'}{r}\right)'\right] \quad (2.9)$$

where  $k = 0$  is for Eq.(2.8a) and  $k \neq 0$  is for Eq.(2.8b). The solution of Eq. (2.9) for  $\gamma \neq 0$  yields,

$$R(r) = ar^2 e^{-\frac{1}{8}\gamma r^2} \quad (2.10)$$

and the solution for  $\gamma = 0$  yields

$$R(r) = ar^2 - b, \text{ or} \quad (2.11a)$$

$$R(r) = ae^{-cr^2} \quad (2.11b)$$

where  $a$ ,  $b$  and  $c$  are complex constants. And the solution Eq.(2.11b) is independent to Eq.(2.11a) under the condition of  $\gamma = 0$ , as the function Eq.(2.9) is nonlinear. Accordingly, by integrating Eq.(2.5) with Eq.(2.10) the pressure is,

$$p(r, z) = \rho H^2(d - 4R^2) - \rho Q(r) \quad (2.12)$$

Thus, Eq.(2.2) with Eq.(2.8) and Eq.(2.10) or Eq.(2.11) give the exact solutions of the flow velocity. It is obvious that there are three independent parameters (e.g.,  $a$ ,  $k$ ,  $\lambda$ ) in the solutions. And other new solutions can also be obtained by combining the different solution at different regions, like that of the Rankine vortex.

### 3. Special solutions

As we know, the Euler equations are defined in the real field. While the above general solutions are defined in the complex field. If the parameters in the solutions are real, the solutions are real. If the parameters are complex, we should try to take the real part of the complex as the solution. However, such approach can not work in general (some additional conditions are required), in that the Euler equations are nonlinear. Such kind of property is common for nonlinear equations, even for a simple nonlinear algebra equation. This problem is similar to the previously mentioned one in Frewer *et al.* (2007), who also found out not all the Lie-algebra solutions satisfy the Euler equations. In their studies, some additional equations required.

For the velocity, the combination of Eq.(2.8) and Eq.(2.10) or Eq.(2.11) according to Eq.(2.2) gives the solution. However, there are too many parameters (including  $\lambda$ ,  $\alpha$ ,  $\beta$ ,  $\gamma$ ,  $k$ ,  $a$ ,  $b$ ,  $c$ ,  $n$ ) in such solution. Our further investigations also pointed out that Eq.(2.1b) holds only for  $\lambda$  being a real number, i.e.,  $\lambda_i = 0$ . Hence, we restricted our following investigations to  $\alpha = 1$ ,  $\beta = 0$ ,  $a = 1$  and  $b = 0$  without loss of generality. Although such restrictions make the flows to be much more simple, they are not trivial. In the following section, we gave some interesting solutions to show how the fluid flows in such conditions.

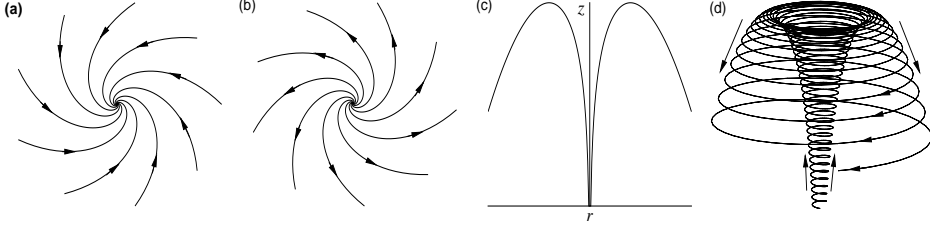


FIGURE 1. Paths of the fluid material elements for the umbrella vortex.

### 3.1. $k \neq 0$

For  $k \neq 0$ ,  $H(z) = e^{kz}$ ,  $\gamma_r = k_r^2 - k_i^2 + \lambda_r^2 - \lambda_i^2$  and  $\gamma_i = 2(k_r k_i + \lambda_r \lambda_i)$ , we have the parameters

$$A_r = (a_r k_r - a_i k_i), B_r = (a_r \lambda_r - a_i \lambda_i), C_r = a_r - \frac{1}{8}(a_r \gamma_r - a_i \gamma_i)r^2 \quad (3.1a)$$

$$A_i = (a_r k_i + a_i k_r), B_i = (a_r \lambda_i + a_i \lambda_r), C_i = a_i - \frac{1}{8}(a_r \gamma_i + a_i \gamma_r)r^2 \quad (3.1b)$$

And the solution is

$$V_r = (A_r \cos \phi - A_i \sin \phi)re^\psi, \quad (3.2a)$$

$$V_\theta = (B_r \cos \phi - B_i \sin \phi)re^\psi, \quad (3.2b)$$

$$V_z = -2(C_r \cos \phi - C_i \sin \phi)e^\psi, \quad (3.2c)$$

where  $\psi = k_r z - \frac{1}{8}\gamma_r r^2$  and  $\phi = k_i z - \frac{1}{8}\gamma_i r^2$ . Although either  $k$  or  $\gamma$  might be complex number, only some especial combinations could be the solutions. The first two types require  $\gamma_i = 0$ , in one case the magnitude of the circular velocity  $V_\theta$  can be either less or larger than that of the radial velocity  $V_r$ , and in another case the magnitude of  $V_\theta$  is larger than that of  $V_r$ . Both suit for typhoon structure. The last two types require  $\gamma_r = 0$ , where the magnitude of  $V_\theta$  is less than that of  $V_r$ .

#### 3.1.1. $k_r \neq 0, k_i = 0$ and $\gamma_i = 0$

In this case  $\gamma$  is a real number with  $\gamma_r > 0$ , and  $k_i = 0$  implies a exponential changes in  $z$ ,

$$V_r = k_r r e^{k_r z - \frac{1}{8}\gamma_r r^2}, \quad (3.3a)$$

$$V_\theta = \lambda_r r e^{k_r z - \frac{1}{8}\gamma_r r^2}, \quad (3.3b)$$

$$V_z = -2\left(1 - \frac{1}{8}\gamma_r r^2\right)e^{k_r z - \frac{1}{8}\gamma_r r^2}. \quad (3.3c)$$

The solution is finite within the whole domain, if we choose appropriate  $k_r > 0$  for  $z < 0$  and  $k_r < 0$  for  $z > 0$ . The circular velocity  $V_\theta$  is the same with that of the Taylor vortex for any fixed  $z$ . The circular velocity maximum is  $V_{\theta m} = \lambda_r r_m e^{k_r z - 1/2}$  at  $r_m^2 = 4/\gamma_r$ . And the vertical velocity  $V_z$  changes it direction at  $r_k^2 = 8/\gamma_r$ , which we call as the radius of vortex kernel  $r_k$ . Such vertical velocity distribution is something like that of the Sullivan vortex (Tong *et al.* 1994; Wu *et al.* 2006). The paths of the fluid material elements are illuminated in Fig 1. In  $r - \theta$  plane, the paths are cyclonic logarithmic spirals (Fig.1a) or anticyclonic logarithmic spirals (Fig.1b) with  $\ln r = k_r \theta / \lambda_r$ . In  $z - r$  plan (Fig.1c), the fluid material element moves spirally along the surface decided by  $z = (\frac{1}{8}\gamma_r r^2 - 2 \ln r) / k_r + const$ . Figure 1d also shows the path in the 3D space. In the inner region  $r < r_k$ , the flow cyclonically ascends from below to above as shown by

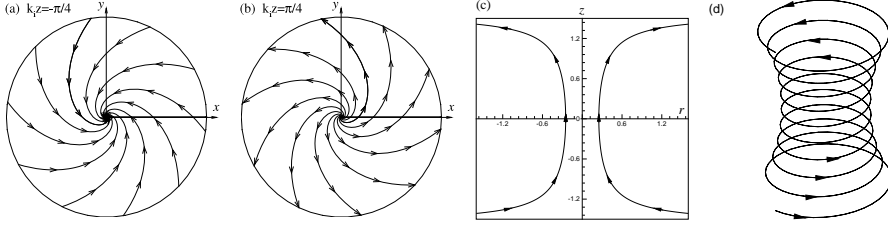


FIGURE 2. Paths of the fluid material elements for multi-planer vortex within a layer.

upward arrow. In the outer region  $r > r_k$ , the descends apart from the kernel. So the mass conserves in this case.

$$\frac{2\pi r_k^2}{e} e^{k_r z} = - \int_0^{r_k} 2\pi r V_z dr = \int_{r_k}^{\infty} 2\pi r V_z dr \quad (3.4)$$

There are two intrinsic length scale in the solution. One is the radius of maximum circular velocity  $r_m$ , the other is the radius of the vortex kernel  $r_k = \sqrt{2}r_m$ . According to the shape of the paths, we called it the umbrella vortex. This new vortex solution is very like that of the typhoon structure, which we know quite limited about.

### 3.1.2. $k_r = 0$ , $k_i \neq 0$ and $\gamma_i = 0$

In this case  $\gamma$  is a real number with  $\gamma_r > 0$  ( $\lambda_r^2 > k_i^2$ ), and  $k_r = 0$  implies a sinusoid function for  $z$  by taking  $k_i > 0$  without loss of generality,

$$V_r = -k_i \sin(k_i z) r e^{-\frac{1}{8}\gamma_r r^2}, \quad (3.5a)$$

$$V_\theta = \lambda_r \cos(k_i z) r e^{-\frac{1}{8}\gamma_r r^2}, \quad (3.5b)$$

$$V_z = -2\left(1 - \frac{1}{8}\gamma_r r^2\right) \cos(k_i z) e^{-\frac{1}{8}\gamma_r r^2}. \quad (3.5c)$$

Similar to the above solution, Eq.(3.5) is finite within the whole domain. But the present solution has multiply layers by noting that the solution is periodic in  $z$ -coordinate. The fluid material elements are restricted within different vertical layers. So we call such flow as multi-planar flow. In each layer (e.g.,  $-\frac{\pi}{2} \leq k_i z \leq \frac{\pi}{2}$ ), the flow has a similar behavior like that in Eq.(3.3), except for that there are both inflow ( $k_i z > 0$ ) and outflow ( $k_i z < 0$ ) at present solution. A similar flow path of the fluid element can be find in Fig.1. There are also two intrinsic length scale in the solution. One is the radius of maximum circular velocity  $r_m$ , the other is the radius of the vortex kernel  $r_k = \sqrt{2}r_m$ . Another notable property of the multi-planar solution is that there might be numberless solutions for a given boundary condition at  $z$ -coordinate. So the solution of the 3D Euler equations for a given boundary condition might not be uniqueness.

### 3.1.3. $k_r = 0$ , $k_i = \pm\lambda_r$ and $\gamma_r = 0$

In this case,  $\gamma_r = \gamma_i = 0$ , the magnitude of  $V_r$  is the same with that of  $V_\theta$  (like Ekman spiral). And the solution of  $R$  is Eq.(2.11) for  $\gamma = 0$ . In Eq.(2.11a), the solution is finite for inner kernel  $r < r_k$  but infinite for far region  $r \rightarrow \infty$ . While in Eq.(2.11b), the solution is finite for far region  $r > r_k$  but infinite for  $r \rightarrow 0$ . Similar to the solution of the Rankine vortex, we can combine the above solutions to obtain a uniform solution at the interface  $r = r_i$ , which is finite at whole region. However, either radial velocity  $V_r$  or the vertical velocity  $V_z$  might be discontinued in Eq.(3.6). Additional notation for  $r_k$  will be given in § 3.2.2.

For example, we choose  $V_r$  to be continued at the interface  $r_i^2 = e^{-cr_i^2} = 1/c$ , hence

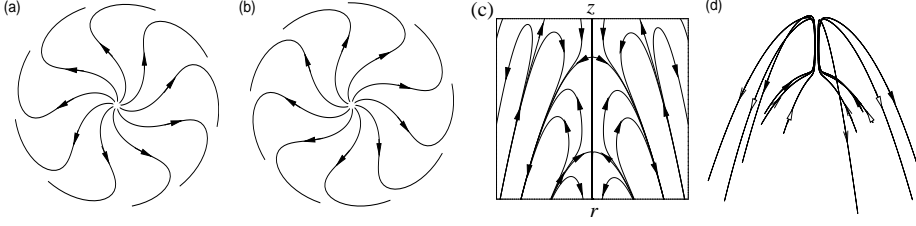


FIGURE 3. Paths of the fluid material elements for multi-paraboloid vortex.

the solution is,

$$V_r = k_i r \sin(k_i z), \quad V_\theta = \pm k_i r \cos(k_i z), \quad V_z = 2 \cos(k_i z) \quad (3.6a)$$

$$V_r = \frac{k_i}{r} e^{-cr^2} \sin(k_i z), \quad V_\theta = \pm \frac{k_i}{r} e^{-cr^2} \cos(k_i z), \quad V_z = -2ce^{-cr^2} \cos(k_i z). \quad (3.6b)$$

The present solution has same function as Eq.(3.5) in  $z$ -coordinate. Besides, the velocities change their directions along the  $r$ -coordinate, which is like that in Eq.(3.5). Figure 2 shows the path of a fluid material element within  $-\pi/2 \leq k_i z \leq \pi/2$  for Eq.(3.6a). According to Eq.(2.3), in  $r - \theta$  plan, the paths are logarithmic spirals  $\ln r = \tan(k_i z)\theta$  (Fig.2a,b). In  $z - r$  plan (Fig.2c), the fluid material element moves spirally along the surface decided by  $\cos(k_i z)r^2 = \text{const}$ . Figure 2d also shows the path in the 3D space. It should be noted that the flow field is respectively inflow and outflow at lower part  $-\pi/2 \leq k_i z \leq 0$  (Fig.2a) and higher part  $0 \leq k_i z \leq \pi/2$  (Fig.2b). However, the path of the fluid material element is always cyclonic from below to above (Fig.2d).

The radial velocity  $V_r$  and the circular velocity  $V_\theta$  continue, but the vertical velocity  $V_z$  discontinue at  $r = r_i$ . If the flow within the inner kernel ascends at  $r < r_i$ , then the flow descends at  $r > r_i$ . The total updraft mass is equal to the total downdraft mass.

$$2\pi r_i^2 \cos(k_i z) = \int_0^{r_i} 2\pi r V_z dr = - \int_{r_i}^{\infty} 2\pi r V_z dr \quad (3.7)$$

#### 3.1.4. $k_r \neq 0$ , $k_i \neq 0$ and $\gamma_r = 0$

In this case  $\gamma$  is a pure image number, and  $\gamma_r = 0$  implies  $k_r^2 - k_i^2 + \lambda_r^2 = 0$ . The solution is,

$$V_r = [k_r \cos(k_i z - \frac{1}{8}\gamma_i r^2) - k_i \sin(k_i z - \frac{1}{8}\gamma_i r^2)] r e^{k_r z}, \quad (3.8a)$$

$$V_\theta = \lambda_r \cos(k_i z - \frac{1}{8}\gamma_i r^2) r e^{k_r z}, \quad (3.8b)$$

$$V_z = -2[\cos(k_i z - \frac{1}{8}\gamma_i r^2) + \frac{\gamma_i}{8} r^2 \sin(k_i z - \frac{1}{8}\gamma_i r^2)] e^{k_r z}. \quad (3.8c)$$

It is obvious that this solution can only be an inner solution  $r < r_k$ , as they might be infinity for  $r \rightarrow \infty$ . In this case, the magnitude of  $V_r$  is  $\sqrt{k_r^2 + k_i^2}$ , which is larger than that of  $V_\theta$ . So the rotation is relatively small, which can be seen from Fig.3a,b. Both the radio velocity and azimuth velocity may change directions along the  $r$ -coordination and  $z$ -coordination. The solution is also a multi-paraboloid vortex by noting that the velocities are spatially periodic shift along the paraboloid of  $k_i z = \frac{1}{8}\gamma_i r^2$  (Fig.3c). For example, Fig.3d depicts the the paths of the fluid material elements within a paraboloid layer. Due to the smaller azimuth velocity, the paths only have some slight twists, whereas there are lots of spirals in Fig.1.

3.2.  $k = 0$ 

In this case, let  $H(z) = z^n$ ,  $n = 0, 1, 2$ . As the solution may be infinity for  $n = 1, 2$  as  $z \rightarrow \infty$ , so it should be taken only as a solution in lower layer  $z < \infty$ .

3.2.1.  $H(z) = 1$ 

Firstly, considering  $n = 0$  and  $H(z) = 1$ , the radial velocity  $V_r$  vanishes according to Eq.(2.2). This is barotropic flows in the geophysics, as the solution is free of  $z$ -coordinate. Any differentiable function  $R(r)$ , the circular velocity  $V_\theta$  and vertical velocity  $V_z$  would be the solution from Eq.(2.6) due to that  $V_\theta$  and  $V_z$  are decoupled for  $H(z) = 1$ , which is known as a stretch-free inviscid vortex can have arbitrary radial dependence (Wu *et al.* 2006). In present solution,  $V_\theta$  and  $V_z$  does not fully decoupled, as Eq.(3.9) shows.

$$V_r = 0, \quad V_\theta = \lambda \frac{R(r)}{r}, \quad V_z = -\frac{R'(r)}{r} \quad (3.9)$$

Given  $R(r) = 1$  is the line vortex,  $R(r) = r^2$  is the solid rotation. And the Rankine vortex and the Taylor vortex can be obtained by given  $R(r) = ar^2 + b$  and  $R(r) = r^2 e^{-ar^2}$ , respectively. The Batchelor vortex and Oseen-Lamb vortex can also be obtained by given  $R(r) = 1 - e^{-r^2}$ , etc (Wu *et al.* 2006).

Although any differentiable function  $R(r)$  gives the vortex solution, not all the vortex can be hold due to the instabilities, including the centrifugal instability and the shear instability (Criminale *et al.* 2003; Wu *et al.* 2006; Sun 2006). In Sun (2006), a general stability criterion was obtained for such circular flows. It was found that the longwaves (e.g. wavenumbers are 1, 2, etc.) might be unstable and break into asymmetrical vortices if there is a local maximum in vorticity distribution along the radial coordinate. The numerical simulations also approved this (Roger *et al.* 1990; Belotserkovskii *et al.* 2009).

3.2.2.  $H(z) = z$ 

Secondly, consider  $n = 1$  and  $H(z) = z$ . If  $\lambda \neq 0$ , the solution is,

$$V_r = are^{-\frac{1}{8}\lambda^2 r^2}, \quad V_\theta = a\lambda re^{-\frac{1}{8}\lambda^2 r^2} z, \quad V_z = -2a(1 - \frac{1}{8}\lambda^2 r^2)e^{-\frac{1}{8}\lambda^2 r^2} z \quad (3.10)$$

And if  $\lambda = 0$ , the circular velocity  $V_\theta$  vanish due to this. Similar to Eq.(3.6), the present solution Eq.(3.11) is also the combination of two parts at  $r = r_i$ , where a discontinuity might occur. One should note that we have chosen  $a = b = 1$  and  $c = 1/r_i^2$  in Eq.(3.6). Hence, the solution for for the whole domain is,

$$V_r = ar, \quad V_\theta = 0, \quad V_z = -2az \quad (3.11a)$$

$$V_r = \frac{b}{r}e^{-cr^2}, \quad V_\theta = 0, \quad V_z = 2bcze^{-cr^2} \quad (3.11b)$$

The vertical velocity  $V_z$  discontinue at  $r = r_i$ , and the vertical velocity discontinuity is  $\Delta V_z = 2a(1 + br_i^2)$ . Similarly, we can choose  $a = -bce^{-cr_i^2}$ , thus the vertical velocity is continued but the radial velocity has a discontinuity of  $\Delta V_r = a(c/r_i + r_i)$ , which is also a two-cell vortex.

3.2.3.  $H(z) = z^2$ 

Finally, consider  $n = 2$  and  $H(z) = z^2$ . As  $\gamma = 0$  implies  $\lambda = 0$ , the circular velocity  $V_\theta$  vanish due to this. Only  $R = r^2$  could satisfy Eq.(2.6), and the solution is,

$$V_r = 2rz, \quad V_\theta = 0, \quad V_z = -2z^2 \quad (3.12)$$

This is the solution of rotational stagnation flow over a plate (Wang 1991), or the Hill spherical vortex (Batchelor 1967; Tong *et al.* 1994; Wu *et al.* 2006).

## 4. Discussion

### 4.1. Extensions of Solutions

In above section, we assumed  $b = 0$  in Eq.(2.11a) to obtain the inner solution. Alternatively, we can take  $a = 0$  and  $b \neq 0$  to as a outer solution, which is a well-known pure vortex solution for stretch-free vortex (Wu *et al.* 2006). It is obvious that Eq.(2.11a) is the solution of the Couette-Taylor flow, we can also use Eq.(2.11a) and  $H(z)$  to obtain new solutions.

In Eq.(3.5) and Eq.(3.6), both solutions have a same  $z$ -coordinate dependence function, so these solutions can also be combined for some new solutions. For example, if we take Eq.(3.5) for  $r < r_i$  and Eq.(3.6b) for  $r > r_i$  as a new solution, where  $r_i^2 = 1/(\frac{2c}{8} - 1)$  and  $c = (1 - \frac{2c}{8})/(3 + \frac{2c}{8})$  in Eq.(3.6b), both the  $V_r$  and  $\partial V_r/\partial r$  of the new combined solution are continued at  $r = r_i$ . As this new solution is continued, it might be better than that of discontinued solution in Eq.(3.6). It is noted that the value of  $\gamma_r$  could be negative in the near-kernel region for present solution, although the solution of Eq.(3.5) requires  $\gamma_r > 0$  in the far region. The negative  $\gamma_r$  implies a very fast tangential velocity rise in the near-kernel region, which is true in the typhoon.

According to the previous studies (Batchelor 1967; Frewer *et al.* 2007), the solution set is quite large, which can also be seen from the Eq.(2.2). According to Batchelor (1967), the vertical velocity  $V_\theta = C(\Psi)/r$ , while we simply took the velocity components as a form  $V_\theta = \lambda\Psi/r$  in Eq.(2.2). Beyond present study, there should be other axisymmetric solutions. For example, we can apply the same approach to find other exact solutions by taking  $V_\theta = \lambda/r$  or  $V_\theta = \lambda\Psi^2(r, z)/r$ , etc. The method used in present work could also be applied to other complex flows, e.g., the geophysical flow in a rotating frame ( $f$ -plane), the magnetohydrodynamics (MHD) in astrophysics, and even for the viscous flows. According to Wang (1991), the generalized Beltrami flow might also be the steady solution of Navier-Stokes equations, if the curl of vorticity is potential. Moreover, the present solutions might further be used to obtain non-steady solutions of Navier-Stokes equations, like that of Oseen-Lamb vortex.

### 4.2. Possible Applications

As mentioned above, a stretch-free inviscid vortex (two-dimensional axisymmetric columnar vortex) can have arbitrary radial dependence for  $H(z) = 1$  (Wu *et al.* 2006). However, many well-known vortex solutions are always similar to either Eq.(2.11a) or Eq.(2.11b). It is from this study that these two-dimensional axisymmetric columnar vortices are also the three-dimensional axisymmetric columnar vortex solutions. So we can find either the Rankine or Taylor vortex for any fixed layer  $z = const$ .

As some new exact solutions are finite within the whole region, they can be applied to study the radial structure of the typhoons, the tornados and the mesoscale eddies in the geophysical flows. As mentioned above, there are 3 independent parameters in the solution. To determinate them, we need the measurable qualities, such as the radius of circular velocity maximum  $r_m$ , the maximum circular velocity  $V_{\theta m}$ , the spiral angle defined by  $k/\lambda$ , the descend/ascend flow mass in Eq.(3.4) and Eq.(3.7), the horizontal inflow/outflow mass (which can also be determined by both  $k/\lambda$  and the descend/ascend flow mass), the angular momentum  $m$ , etc. According to Eq.(2.2), the angular momentum  $m = rV_\theta = -\lambda R(r)H(z)$ , thus the solutions of  $R(r)$  (Eq.(2.10) and Eq.(2.11)) can be applied to discuss the angular momentum of the vortex. For the typhoon observations, such solutions can be used to fit the real velocity distribution along the radial coordinate. This may also be useful to classify the typhoons and the tornados according the flow structures provided by above solutions.

## 5. Conclusion

A general exact axisymmetric spiral solution was obtained for 3D incompressible Euler equations, and some exact solutions were also obtained. The solution describes the spiral path of the fluid material element on the Bernoulli surface. The explicit umbrella vortex and multi-layer vortex solutions, which are new in this investigation, might be used to describe the 3D structure of the tropical cyclones, tornados and mesoscale eddies in the geophysical flows. The solutions also imply that the spiral structure is the intrinsic structure of the flows in the nature.

The method used in present work is very straightforward, and it could also be applied to other complex flows, e.g., the geophysical flows in a rotating frame ( $f$ -plane), and even for the non-steady viscous flows.

The author thanks Prof. Wang W. at OUC, who discussed lots of vortex dynamic problems with the author and encouraged the author to finish this work. The author also thanks Dr. Wang Bo-fu and Dr. Wan Zhen-hua for their help to check the formula, Prof. Huang Rui-Xin at WHOI for useful comments. Prof. Yin X-Y at USTC is also acknowledged, who led the author to this field. This work is supported by the National Basic Research Program of China (No. 2007CB816004), and the Knowledge Innovation Program of the Chinese Academy of Sciences (Nos. KZCX2-YW-QN514).

## REFERENCES

- BATCHELOR, G. K. 1967 *An Introduction to Fluid Dynamics*. Cambridge, U. K.: Cambridge University Press.
- BELOTSERKOVSKII, O.M., DENISENKO, V.V., KONYUKHOV, A.V., OPARIN, A.M., TROSHKIN, O.V. & CHECHETKIN, V.M. 2009 Numerical stability analysis of the taylorcouette flow in the two-dimensional case. *Computational Mathematics and Mathematical Physics* **49**(4), 729–742.
- CRIMINALE, W. O., JACKSON, T. L. & JOSLIN, R. D. 2003 *Theory and computation of hydrodynamic stability*. Cambridge, U.K.: Cambridge University Press.
- FREWER, M., OBERLACK, M. & GUENTHER, S. 2007 Symmetry investigations on the incompressible stationary axisymmetric euler equations with swirl. *Fluid Dyn. Res.* **39**, 647–664.
- LONG, R. R. 1958 Vortex motion in a viscous fluid. *J. Meteorol.* **15**, 108–112.
- LONG, R. R. 1961 A vortex in an infinite viscous fluid. *J. Fluid Mech.* **11**, 611–624.
- LOU, S. Y., JIA, M., TANG, X. & HUANG, F. 2007 Vortices, circumfluence, symmetry groups, and darbox transformations of the 2+1-dimensional euler equation, **75**, 056318.
- MAJDA, A. J. & BERTOZZI, A. L. 2002 *Vorticity and Incompressible Flow*. Cambridge University Press.
- MOFFATT, K. 1969 The degree of knottedness of tangled vortex lines. *J. Fluid Mech.* **35**, 117–129.
- ROGER, K. S., WOLFGANG, U. & GRAY, D. 1990 A numerical study of tropic cyclone motion using a barotropic model. Part I: the role of vortex asymmetrics. *Quart. J. Roy. Meteor. Soc.* **116**, 337–362.
- SAFFMAN, P. G. 1992 *Vortex Dynamics*. Cambridge, U.K.: Cambridge University Press.
- SHTERN, V., BORISSOV, A. & HUSSAIN, F. 1997 Vortex sink with axial flow: solution and applications. *Phys. Fluids* **9**, 2941–2959.
- SHTERN, V. & HUSSAIN, F. 1999 Collapse, symmetry breaking, and hysteresis in swirling flows. *Ann. Rev. Fluid Mech.* **31**, 537–566.
- SUN, L. 2006 General stability criteria for inviscid rotating flow. *arXiv:physics/0603177v1*.
- SUN, L. 2011 A typhoon-like vortex solution of incompressible 3D inviscid flow. *Theor. Appl. Mech. Lett.* **1** (4), 042003.
- TONG, B.G., YIN, X.Y. & ZHU, K.Q. 1994 *Theory of Vortex Motion*. Hefei, China: University of Science and Technology of China Press.
- WANG, C. Y. 1991 Exact solutions of the steady-state navier-stokes equations. *Ann. Rev. Fluid Mech.* **23**, 159–177.

WU, J. Z., MA, H. Y. & ZHOU, M. D. 2006 *Vorticity and Vortex Dynamics*. Berlin Heidelberg, Germany: Springer.